Experimental Evaluation of Fatigue Damage Progression in Postbuckled Single Stringer Composite Specimens

Authors: Chiara Bisagni Carlos G. Dávila Cheryl A. Rose Joseph N. Zalameda

ABSTRACT

The durability and damage tolerance of postbuckled composite structures are not yet completely understood, and remain difficult to predict due to the nonlinearity of the geometric response and its interaction with local damage modes. A research effort was conducted to investigate experimentally the quasi-static and fatigue damage progression in a single-stringer compression (SSC) specimen. Three specimens were manufactured with a hat-stiffener, and an initial defect was introduced with a Teflon film embedded between one flange of the stringer and the skin. One of the specimens was tested under quasi-static compressive loading, while the remaining two specimens were tested by cycling in postbuckling.

The tests were performed at the NASA Langley Research Center under controlled conditions and with instrumentation that allows a precise evaluation of the postbuckling response and of the damage modes. Three-dimensional digital image correlation VIC-3D systems were used to provide full field displacements and strains on the skin and the stringer. Passive thermal monitoring was conducted during the fatigue tests using an infrared camera that showed the location of the delamination front while the specimen was being cycled. The live information from the thermography was used to stop the fatigue tests at critical stages of the damage evolution to allow detailed ultrasonic scans.

INTRODUCTION

Composite stiffened panels used in aerospace structures can sustain loads far in excess of their buckling loads. The collapse of stiffened panels is generally observed deep into the postbuckling range, and is usually due to the interaction of the

Chiara Bisagni, University of California San Diego, Department of Structural Engineering, 9500 Gilman Drive #0085, La Jolla, CA, 92093-0085
Carlos G. Dávila and Cheryl A. Rose, NASA Langley Research Center, Structural Mechanics and Concepts Branch, Hampton, 23681 VA, USA
Joseph N. Zalameda, NASA Langley Research Center, Nondestructive Evaluation Services Branch, Hampton, 23681 VA, USA

postbuckling deformations with local damage modes, in particular skin/stringer disbonding.

The need to understand the postbuckling response of thin stiffened structures has long been recognized. Although the high cost of manufacturing prototype composite structures and the difficulty to set up high fidelity tests with a complete set of measurements make these tests quite complex and expensive to execute, several sources of well-documented experimental results describing the postbuckling response and collapse of composite stiffened structures are available in the literature [1-8].

Fewer tests are reported regarding the response of stiffened structures subjected to fatigue loads in the postbuckling range [9-10]. For fatigue loading conditions the problem is more complex due to interaction between the nonlinearity of the geometric response, the different possible damage modes, and the accumulation of cyclic damage. These tests are also expensive to conduct due to the length of time that is required.

For these reasons, a Single Stringer Compression (SSC) specimen was developed previously by the authors to study the response and the failure of a multi-stringer panel loaded in compression [11-12]. The present investigation relies on the results of two previous test campaigns performed by the authors. The first one, conducted at the Politecnico di Milano, was used mainly to verify the design of the SSC specimen, and to develop a progressive damage analysis capable of predicting the initiation and propagation of skin/stiffener debonding as well as the damage mechanisms that cause crippling of the stringer [12-13]. The second test campaign was conducted at the NASA Langley Research Center. Before the tests, the specimens were subjected to ultrasonic (UT) scans to ensure that they were free of manufacturing defects. Their initial deformations were also carefully measured in a Coordinate Measurement Machine (CMM). Three-dimensional digital image correlation (DIC) was used to monitor the formation and evolution of the postbuckling deformations. A high-speed camera capturing 16,000 frames per second was used to understand the collapse sequence [14].

The work presented herein describes the last test campaign performed by the authors and the results obtained. The tests were conducted at the NASA Langley Research Center and they focused on the evolution of damage in SSC specimens cycled into postbuckling. The specimens were manufactured with a co-cured hat-stiffener and an initial defect was introduced with a Teflon film embedded between one flange of the stringer and the skin. Three dimensional digital image correlation was used to monitor the deformation response, and passive infrared thermography was used to capture damage evolution while the specimen was being cycled. Information obtained from the thermography was used to guide test interruption for more detailed evaluation of the damage evolution using in-situ high-resolution ultrasonic scans.

SINGLE STRINGER COMPRESSION SPECIMEN

In previous numerical/experimental investigations a single-stringer compression (SSC) specimen was developed by the authors to study the postbuckling and failure response of a multi-stringer panel loaded in compression [11-14]. The SSC specimen represents a small portion of a multi-stringer panel and was designed to have similar response characteristics as the corresponding multi-stringer panel. The SSC specimen

represents an intermediate level of complexity between coupon-level specimens and structural components while exhibiting most of the challenges that characterize the assessment of the damage behavior of a more complex multi-stringer panel. The damage tolerance of SSC specimens is investigated by placing a Teflon insert between the stringer and the skin during manufacturing. The SSC specimen is advantageous from an experimental point of view, because of relatively low manufacturing and testing costs, and from a numerical point of view, because of moderate computational model size requirements.

The configuration of the SSC specimen investigated is shown in Figure 1, where all dimensions shown are in mm. The specimen is composed of one hat-stringer, with the skin and stringer co-cured. The height of the stringer is 30 mm, the width of the crown top is 15 mm, and the stiffener flange width is 15 mm. The entire specimen is made of IM7/8552 graphite epoxy material. The skin is an 8-ply quasi-isotropic laminate with a stacking sequence of $[45°/90°/-45°/0°]_S$ for a total thickness of 1 mm. The stringers are composed of a 7-ply laminate with a symmetric stacking sequence of [-45°/0°/45°/0°/45°/0°/-45°] which results in a total thickness of 0.875 mm. An initial defect was introduced at the specimen mid-length, by placing a 40-mm-long Teflon film between one flange of the stringer and the skin.

In the previous work [12], geometrically nonlinear analyses of a multi-stringer panel were used to identify repeating features in the predicted response that characterize the response of the multi-stringer panel. The dimensions of a single stringer panel whose response is similar to the multi-stringer panel, in terms of postbuckling deformation and failure mechanisms, were then determined. For the particular multi-stringer panel that was considered, it was determined that a single stringer panel with length equal to 240 mm and width equal to 150 mm, as shown in Figure 1, best matched the response of the multi-stringer panel.

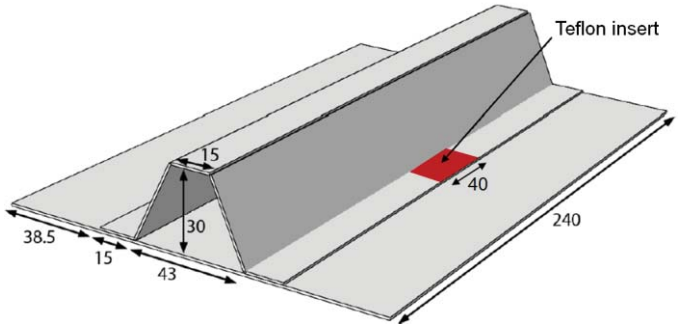

Figure 1. Single-stringer compression (SSC) specimen. (All dimensions in mm.).

The specimens were encased in potting at the two ends by means of two 30 mm long tabs cast with a mixture of epoxy resin and aluminum powder. The tabs ensure a uniform distribution of the load during the tests. For experimental simplicity, the longitudinal edges of the SSC specimen are free, while the corresponding locations of the multi-stringer structure are subjected to the restraining effect of the surrounding structure. This restraining effect results in a membrane stress distribution in the multi-stringer panel that is not exactly the same as the membrane stress distribution that develops in the SSC specimen with free edges. However, comparison of stress distributions in the multi-stringer panel to those in the SSC specimen revealed that, for the particular design under consideration, the skin/stiffener interaction and the

corresponding maximum stress failure index distribution in the proximity of the edge of the stringer flange is similar between the two panels. Consequently, the SSC specimen provides a valid configuration for assessing the damage tolerance of the multi-stringer panel and, at the same time, it can reduce the expense associated with testing larger multi-stringer panels.

EXPERIMENTAL PROCEDURE AND INSTRUMENTATION

Three SSC specimens were tested at the NASA Langley Research Center to study the evolution of damage under quasi-static and cyclic compression loads. A quasi-static test in compression was performed on one of the specimens, and the other two specimens were tested in fatigue by cycling into postbuckling.

The tests were conducted under controlled conditions using an MTS test frame, and with instrumentation that allowed a precise evaluation of the postbuckling response and of the damage evolution. The test frame and the instrumentation used to monitor the structural response and damage propagation during the tests is shown in Figure 2

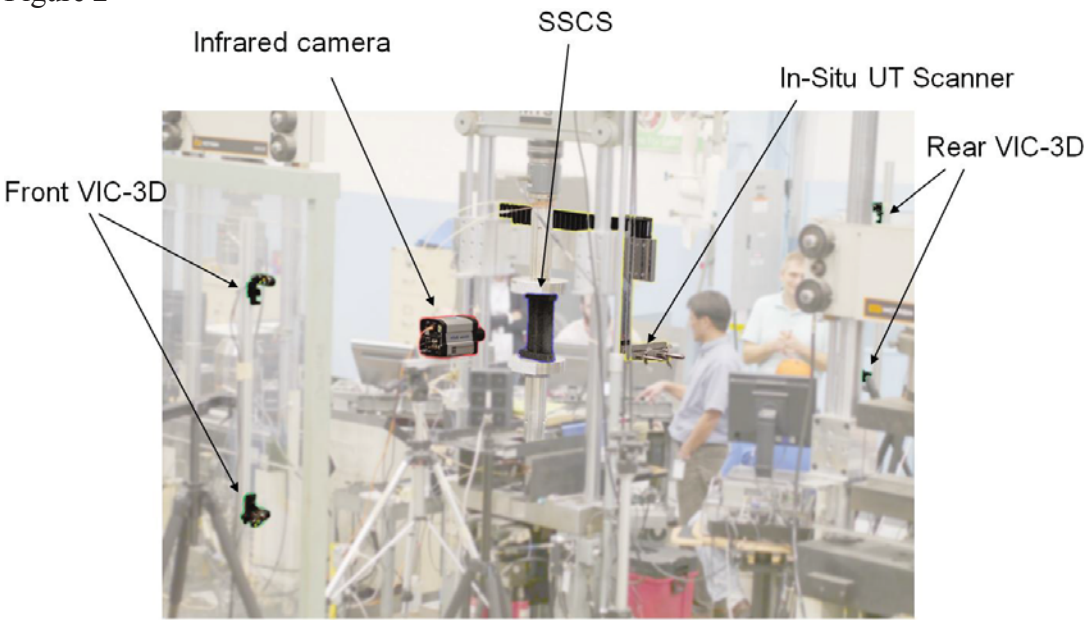

Figure 2. Test frame and instrumentation used to monitor the structural response and damage propagation.

Digital image correlation was used extensively. Two three-dimensional digital image correlation VIC-3D systems [15] were used to monitor the formation and evolution of the postbuckling deformations and to measure the full-field displacements and strains on the skin and on the stringer sides of the specimen.

Passive thermal monitoring was conducted in real time during the fatigue tests using an infrared camera. Inspection by passive thermography is accomplished without the application of external heat. Instead, the rubbing of matrix cracks and delaminations induces heating that is detectable by the infrared camera. The technique is particularly useful in fatigue because it can track the position of a delamination front during fatigue cycling without stopping the test [16]. The live information from the

thermography was used to stop the fatigue tests at critical stages of the damage evolution to allow detailed measurements using a non-immersion in-situ ultrasonic (UT) scanner, i.e. without removing the specimen from the load frame [17]. The in-situ UT scanner probe and the UT scanner translation stage mounted on the load frame are shown in Figure 3.

STATIC TEST

The first specimen was subjected to quasi-static compressive loading under displacement control conditions, with a loading rate of 0.0635 mm/min. Buckling started in the skin as three half-waves along the specimen length. The out-of-plane deformations increased gradually with load. Transition into the postbuckling range was progressive, and it was difficult to identify the buckling load precisely. Nevertheless, the buckling load can be estimated to be about 7 kN, which is when the rate of the out-of-plane deformation increased rapidly.

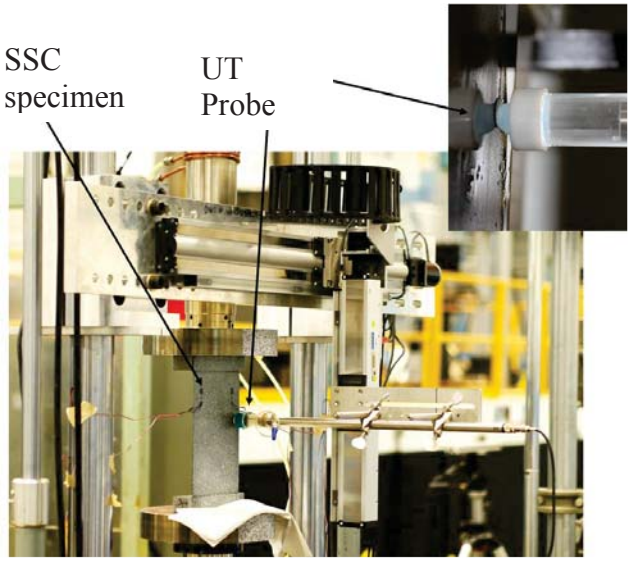

Figure 3. In-situ ultrasonic scanner.

The number of half-waves along the free edges of the skin did not change with increased load, but small waves developed in the central area of the skin under the stiffener. These postbuckling modes originated at applied loads that are higher than those that cause buckling of the free edges of the skin and they are characterized by higher numbers of half-waves. The buckling and the postbuckling behavior were very similar to those observed in the previous test campaign [12].

The ultimate strength of the specimen was equal to 28.46 kN. The postbuckling out-of-plane displacement deformation, *w*, immediately preceding failure is shown in Figure 4, where the measurements taken with the VIC3D systems are reported both on the stringer side of the specimen (Figure 4a) and on the skin side of the specimen (Figure 4b). The out-of-plane displacements of the skin range from 1.3 mm in the direction of the stringer (positive z-direction, stringer side) to 3 mm in the opposite direction. The scales in Figures 4a, 4b, and in subsequent VIC3D figures were selected to highlight the deformation shapes and are different between the skin and the stringer views. The contours are shown for qualitative purposes to illustrate deformation shapes and, therefore, the values of the displacements are not shown on the scale.

Failure produced a sudden opening of the delamination between the stringer flange and skin at the Teflon insert, along with an extension of the initial delamination defect, which caused the load to drop to 24.65 kN. The postbuckling deformations reported on the stringer and skin side of the specimen after the initial defect extension are shown in Figures 5a and b, respectively. The shape of the deformation on the side of the Teflon insert changed significantly compared to the deformation before the growth of the initial defect. The magnitude of the out-of-plane displacements of the skin reached 6.3 mm in the direction opposite to the stringer (positive z-direction as viewed from skin side).

After failure, the specimen was unloaded for a UT scan. The UT scan indicated approximately 30 mm of extension in the longitudinal direction of the initial defect on both sides of the Teflon film, giving a total skin-stringer separation length equal to 100 mm. After the scan, the specimen was reloaded. As the load level approached the previous failure load (28.38 kN), the stringer detached suddenly from the skin, creating a tunnel under the stringer. The corresponding deformation measured with the two VIC3D systems is shown in Figure 6.

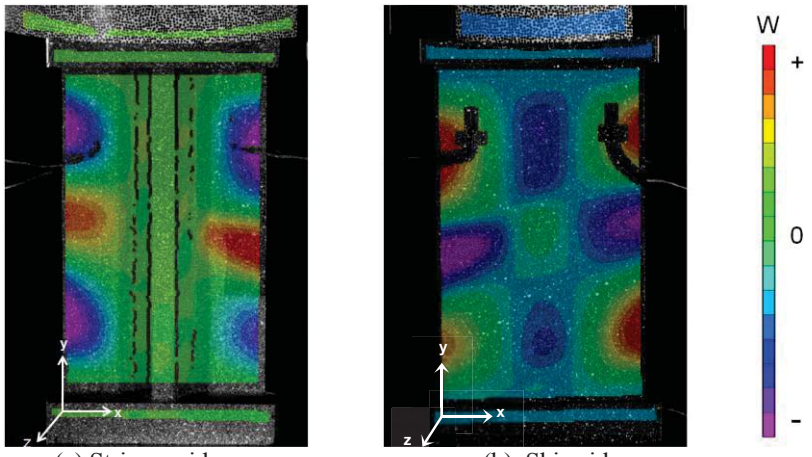

(a) Stringer side (b) Skin side

Figure 4. Postbuckling out-of-plane displacements immediately before opening of Teflon-induced defect. Load = 28.46 kN.

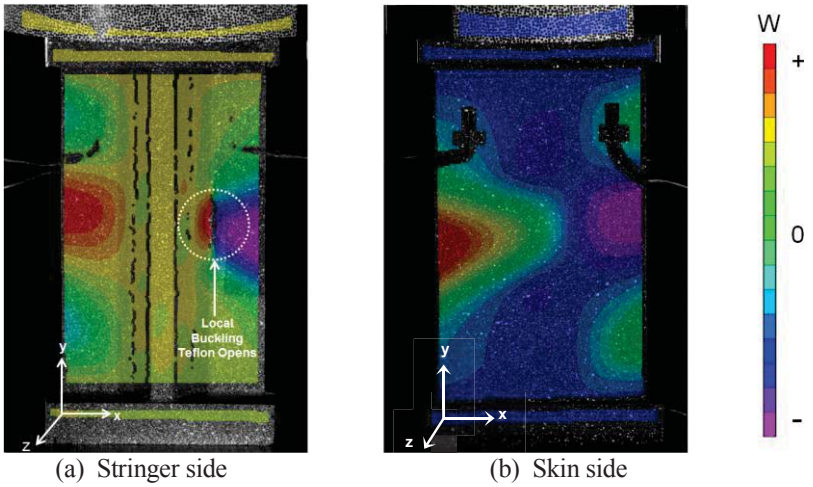

(a) Stringer side (b) Skin side

Figure 5. Postbuckling out-of-plane displacements after opening of the Teflon-induced defect. Load=24.65 kN.

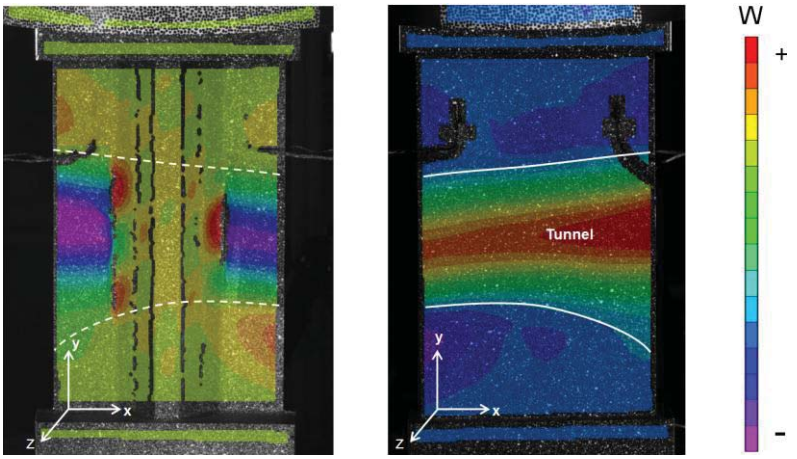

(a) Stringer side (b) Skin side

Figure 6. Postbuckling out-of-plane displacements after tunneling. Load = 21.02 kN.

The load-shortening curves for the static test are shown in Figure 7. The blue curve corresponds to the first compressive loading of the specimen. The peak of the blue curve corresponds to the load at which the Teflon-induced defect snapped open and extended from 40 mm to approximately 100 mm. The red curve corresponds to a reloading of the specimen, and its peak corresponds to the initiation of stringer detachment from the skin, forming a tunnel under the stringer. The reduced stiffness during reloading suggests that the extension of the initial defect at the Teflon insert caused a non-negligible loss of stiffness.

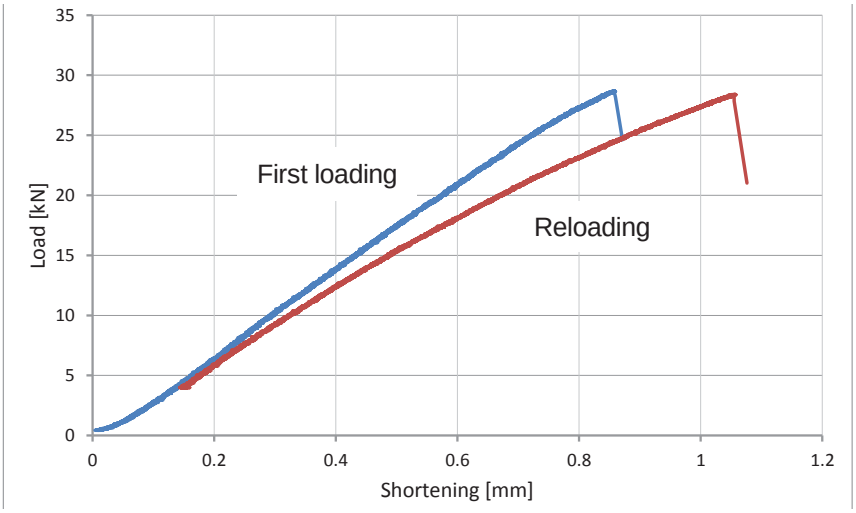

Figure 7. Load-shortening curves of the quasi-static SSC specimen test.

FATIGUE TESTS

Two SSC specimens were tested in fatigue. These specimens were nominally identical to the specimen tested quasi-statically. The analysis conducted before the test

campaign predicted that the initial delamination defect induced by the Teflon insert begins to propagate when the load reaches 80% of the collapse load. Based on this observation, the peak load applied during fatigue testing was equal to 80% of the maximum load measured during the static test. The specimens were loaded in fatigue at 2 Hz, cycling between 2.3 kN and 23 kN.

Digital image correlation was used during cyclic loading to monitor the formation and evolution of the postbuckling deformations. Passive thermography and UT scanning were used to track the evolution of the damage.

Two images captured by the digital image correlation system on the skin side of the panel during one of the first load cycles applied to the first SSC specimen are shown in Figure 8. The postbuckling deformation initiated as three half-waves in the skin (Figure 8a) and then, during the same cycle, a smaller fourth half-wave formed in the skin on the side of the specimen with the Teflon insert (Figure 8b). Small waves also developed in the central area of the skin under the stiffener but cannot be seen in Figure 8b.

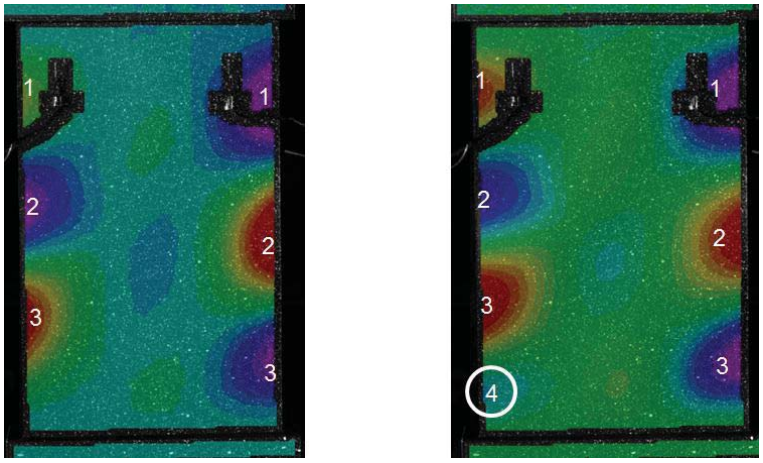

a) Load: 12.88 kN b) Load: 18.08 kN

Figure 8. Evolution of postbuckling mode during cycle #10 of fatigue testing of the first fatigue SSC specimen.

A sudden extension of the initial defect at the Teflon insert was detected with the passive thermography after only 20 cycles. The test was stopped and UT measurements were taken, which confirmed that the initial defect had extended, from the initial Teflon-film insert length of 40 mm to approximately 68 mm. Testing was continued. After 1,000 cycles a UT scan was taken which indicated that no further extension of the disbond had occurred. After a total of 2,000 cycles, a new UT scan indicated that the disbond had propagated from a length of approximately 68 to 72 mm. After 6,750 cycles, a delamination front in the shape of a half-moon on the flange opposite to the initial defect could be observed in the image from the passive thermography, as shown in Figure 9. The test was stopped and another UT scan was taken. The test was then continued until a complete skin-stringer separation occurred at 6,800 cycles.

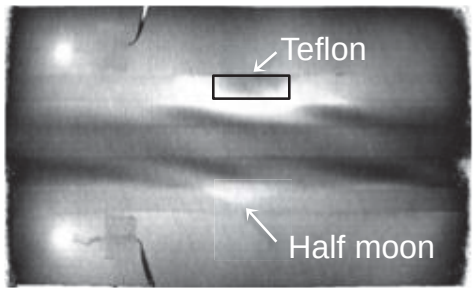

Figure 9. Passive thermography image during testing of the first fatigue SSC specimen, 6750 cycles.

A sequence of three images obtained by the UT measurements at 1000, 2000 and 6750 cycles during the fatigue test are shown in Figures 10a-c, respectively. The images clearly show the extension of the initial skin-stringer separation along the length of the specimen and in the transverse direction as indicated by the half-moon shape disbond extending into the flange opposite to the Teflon insert.

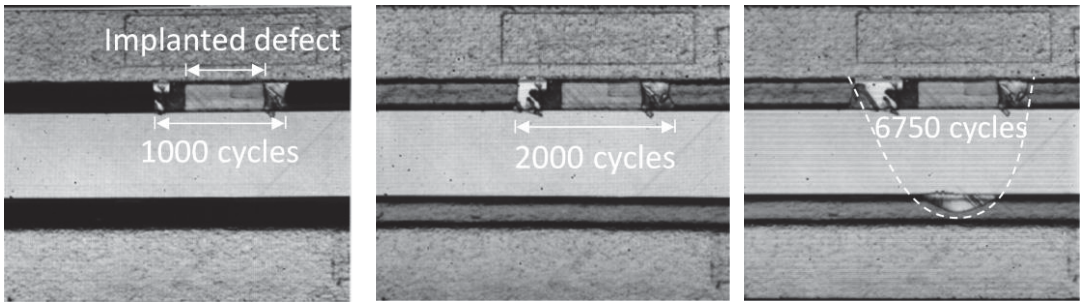

(a) 20-1000 cycles (b) 2000 cycles (c) 6750 cycles

Figure 10. Damage propagation measured by UT scan during fatigue testing of the first SSC specimen.

The measurements taken with the VIC3D system were post-processed and the results indicate a difference between the deformation shapes measured at about 1,000 cycles and at about 6,500 cycles, as can be seen in Figure 11. The out-of-plane deformation obtained with digital image correlation after 1,000 cycles is shown in Figure 11a, and near specimen failure, at 6,500 cycles, in Figure 11b.

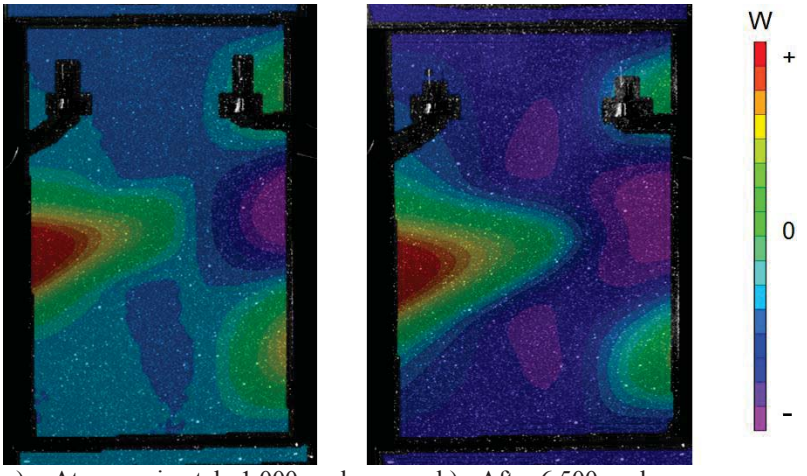

a) At approximately 1,000 cycles b) After 6,500 cycles

Figure 11. Evolution of out-of-plane deformation during fatigue testing of the first SSC fatigue specimen due to progression of skin-stringer separation.

Fatigue testing of the second SSC specimen was initiated using the same loading parameters as used in testing of the first fatigue specimen. At approximately 2,000 cycles, the Teflon-induced defect opened suddenly. Results from a UT scan indicated that the initial defect at the Teflon insert had extended from the initial 40 mm length to a length of 50 mm. The out-of-plane deformation obtained with the digital image correlation just before and after the extension is shown in Figure 12.

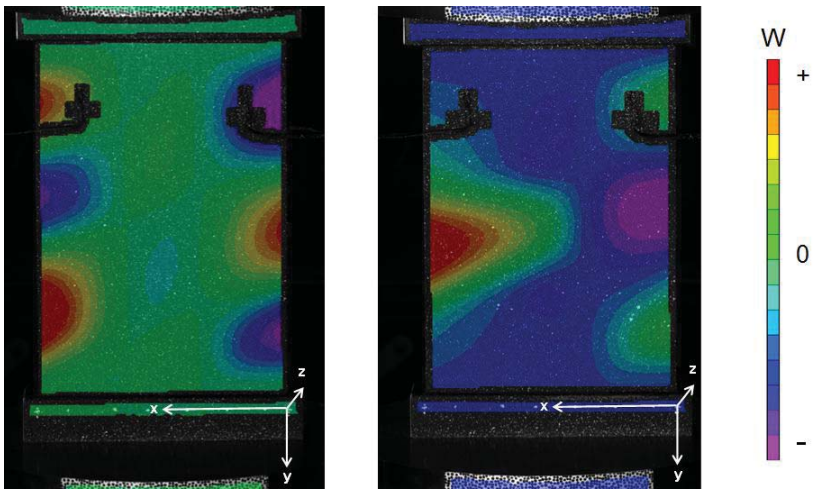

a) At approximately 1,000 cycles b) After 2,500 cycles

Figure 12. Postbuckling mode before and after opening and extension of the initial defect at the Teflon insert, second fatigue SSC specimen.

After 24,000 cycles and several UT measurements that did not reveal any further extension in the skin-stringer separation, the peak load level was increased to 24 kN, which is 85% of the quasi-static strength. Testing was re-started with a cyclic load of 2.4 to 24 kN. At 25,521 cycles the specimen collapsed suddenly due to the separation of the stiffener from the skin for the entire width.

CONCLUDING REMARKS

A series of static and fatigue tests were performed at the NASA Langley Research Center on single stringer compression (SSC) specimens. Three specimens were manufactured with a co-cured hat-stringer, and an initial defect was introduced at the specimen mid-length with a Teflon film embedded between one flange of the stringer and the skin. One of the specimens was tested under quasi-static compressive loading, while the remaining two specimens were tested by cycling in postbuckling. The tests were conducted under controlled conditions and the specimens were monitored throughout the loading with multiple in-situ NDE methods to obtain detailed information on deformation response characteristics and damage evolution. Three-dimensional digital image correlation was used to obtain full-field displacement measurements, and in-situ passive thermography and UT were used to track damage evolution.

The ultimate strength of a SSC specimen was determined with a quasi-static test. Fatigue tests were conducted on two nominally identical specimens, with a peak cyclic

load of 80% of this strength for one specimen and 85% of this strength for the other specimen. Using passive thermography with an infrared camera, it was possible to monitor the growth of the initial delamination defect while the specimens were being cycled. The live information from the thermography was used to determine stopping points along the fatigue tests to ensure that critical stages of the damage evolution were captured by stopping the tests at the required times and performing detailed ultrasonic scans.

After an initial opening and extension of the Teflon-induced embedded defect, the specimens were found to be able to sustain a high number of cycles. It was observed that when a skin-stringer separation develops with the shape of a half-moon in the opposite flange, it propagates rapidly within a small number of cycles and causes the collapse of the specimen. The test results presented herein contribute to a better understanding of the complex response phenomena exhibited by postbuckled stiffened structures subjected to fatigue loads cycling in the postbuckling range.

REFERENCES

1. Singer, J., J. Arbocz, and T. Weller. 2002. *Buckling Experiments, Experimental Methods in Buckling of Thin-Walled Structures*. Vol. 1 and 2. John Wiley & Sons.
2. Abramovich, H., T. Weller, and C. Bisagni. 2008. "Buckling Behavior of Composite Laminated Stiffened Panels under Combined Shear-Axial Compression," *Journal of Aircraft*, 45(2):402-413.
3. Falzon, B.G. 2001. "The Behaviour of Damage Tolerant Hat-Stiffened Composite Panels Loaded in Uniaxial Compression," *Composites Part A: Applied Science and Manufacturing*, 32(9):1255-1262.
4. Ambur D. R., N. Jaunky, and M. W. Hilburger. 2004. "Progressive Failure Studies of Stiffened Panels subjected to Shear Loading," *Composite Structures*, 65:129-142.
5. Ambur, D.R., N. Jaunky, M. Hilburger, and C. G. Dávila. 2004. "Progressive Failure Analyses of Compression-Loaded Composite Curved Panels with and without Cutouts," *Composite Structures*, 65:143-155.
6. Degenhardt R., A. Kling, H. Klein, W. Hillgers, H.C. Goetting, R. Zimmermann, K. Rohwer, and A. Gleiter. 2007. "Experiments on Buckling and Postbuckling of Thin-Walled CFRP Structures using Advanced Measurement Systems," *International Journal of Structural Stability and Dynamics*, 7(2):337-358.
7. Greenhalgh, E., C. Meeks, A. Clarke, and J. Thatcher. 2003. "The Effect of Defects on the Performance of Post-Buckled Stringer-Stiffened Panels," *Composites Part A: Applied Science and Manufacturing*, 34:623-633.
8. Kong, C. W., C. S. Hong, and C. G. Kim. 2002. "Postbuckling Strength of Stiffened Composite Plates with Impact Damage," *AIAA Journal*, 38 (10):1956-1964.
9. Abramovich, H., and T. Weller. 2010. "Repeated Buckling and Postbucking Behavior of Laminated Stringer Stiffened Composite Panels with and without Damage," *International Journal of Structural Stability and Dynamics*, 4:807-825.
10. Cordisco, P., and C. Bisagni. 2011. "Cyclic Buckling Tests under Combined Loading on Pre-Damaged Composite Stiffened Boxes," *AIAA Journal*, 49(8):1795-1807.
11. Bisagni, C. 2006. "Progressive Delamination Analysis of Stiffened Composite Panels in Post-Buckling," in *47th AIAA/ASME/ASCE/ASC Structures, Structural Dynamics, and Materials Conference*, Newport, Rhode Island, USA, 1-4 May 2006, AIAA 2006-2178.
12. Bisagni, C., R. Vescovini, and C. G. Dávila. 2011. "Development of a Single-Stringer Compression Specimen for the Assessment of Damage Tolerance of Postbuckled Structures," *Journal of Aircraft*, 48(2):495-502.

13. Vescovini, R., C. G. Dávila, and C. Bisagni. 2013. “Failure Analysis of Composite Multi-Stringer Panels using Simplified Models,” *Composites: Part B*, 45:939-951.

14. Bisagni, C., and C. G. Dávila. 2014. “Experimental Investigation of the Postbuckling Response and Collapse of a Single-Stringer Specimen,” *Composite Structures*, 108:493-503.

15. VIC-3D. 2010. Software Package, Ver. 2010.1.0, Correlated Solutions, Inc., Columbia, SC.

16. Zalameda, J. N., E. R. Burke, F. R. Parker, J. P. Seebo, C. W. Wright, and J. B. Bly. 2012. “Thermography Inspection for Early Detection of Composite Damage in Structures during Fatigue Loading,” in *SPIE Defense, Security, and Sensing*, 835403-835403-9.

17. Johnston, P.H., C. W. Wright, J. N. Zalameda, and J. P. Seebo JP. 2010. *Ultrasonic Monitoring of Ply Crack and Delamination Formation in Composite Tube under Torsion Load*. NASA Technical Report 20100036748.